

ENHANCING TARGETED TRANSFERABILITY VIA FEATURE SPACE FINE-TUNING

Hui Zeng^{1,2}, Biwei Chen³, and Anjie Peng^{1,2*}

¹Southwest University of Science and Technology

³Beijing Normal University

²Guangdong Provincial Key Laboratory of Information Security Technology

ABSTRACT

Adversarial examples (AEs) have been extensively studied due to their potential for privacy protection and inspiring robust neural networks. However, making a targeted AE transferable across unknown models remains challenging. In this paper, to alleviate the overfitting dilemma common in an AE crafted by existing simple iterative attacks, we propose fine-tuning it in the feature space. Specifically, starting with an AE generated by a baseline attack, we encourage the features that contribute to the target class and discourage the features that contribute to the original class in a middle layer of the source model. Extensive experiments demonstrate that only a few iterations of fine-tuning can boost existing attacks in terms of targeted transferability nontrivially and universally. Our results also verify that the simple iterative attacks can yield comparable or even better transferability than the resource-intensive methods, which rely on training target-specific classifiers or generators with additional data. The code is available at: github.com/zengh5/TA_feature_FT.

Index Terms—adversarial examples, simple iterative attack, fine-tuning, targeted transferability

1. INTRODUCTION

Exploring adversarial examples (AEs) is helpful in demystifying deep neural networks (DNN) [1], identifying the DNN models’ vulnerability [2], and protecting privacy [3]. The attack ability of an AE is usually measured by its transferability, i.e., the chance to fool unseen models. Numerous transferable attacks have emerged recently; for example, advanced algorithms have been adopted to stabilize the optimization direction and prevent AEs from falling into poor local maxima [4–6].

While existing studies have pushed the limit of the transferability under the untargeted mode, few focus on targeted attacks. Targeted transferability is much more challenging since it requires unknown models outputting a specific label [7]. Tailored schemes for improving the transferability of targeted attacks have been proposed to fill the gap. Resource-intensive attacks seek extra, target-specific classifiers [8] or generators [9] to optimize adversarial perturbations. However, when the number of targeted classes is enormous, the training time will be problematic. In contrast, other researchers find that integrating novel loss functions with conventional simple iterative attacks can also enhance targeted transferability [10–12]. Our work falls into this latter category.

The huge gap between the success rates of white-box/black-box targeted attacks suggests that simple iterative attacks heavily overfit the source model. Such a dilemma is not unique to just targeted attacks. In the context of untargeted attacks, apart from the well-known data or model augmentation strategies [13–17], researchers recently resorted to feature space disruption to mitigate the overfitting issue [18–22]. This strategy is based on the observation that early layers (closer to the input) are more class-specific, whereas later layers are more model-specific. Hence, targeting the middle layers may alleviate the overfitting issue and thus enhance transferability.

However, our preliminary experiments show that directly extending feature space attacks to the targeted mode does not work since representing the target class as a single point in an internal layer is difficult. Such a somewhat frustrating result does not mean this idea is not helpful for targeted attacks. In this work, we find that fine-tuning an existing AE in the feature space can further effectively enhance its targeted transferability. Precisely, starting with an AE generated by a baseline attack, we fine-tune it for a few iterations to encourage the target class-associated features and suppress the original class-associated features in an internal layer of the source model. We incorporate the proposed fine-tuning strategy with various state-of-the-art simple iterative attacks. Experiments on ImageNet demonstrate that the targeted transferability of all the considered attacks can be improved notably via a few iterations of feature space fine-tuning.

2. RELATED WORK

2.1. Transferable untargeted attack

An untargeted attack aims to lead a DNN-based classification model $f(\cdot)$ into making a wrong output, i.e., $f(I') \neq f(I)$, where I is the original image and I' is the adversarial one. As a common baseline, the iterative fast gradient sign method (IFGSM) [23] can be formulated as follows:

$$I'_{n+1} = \text{Clip}_{I, \epsilon} \{I'_n + \text{asign}(\nabla_{I'_n} J(I'_n, y_o))\} \quad (1)$$

where $I'_0 = I$, $\nabla_{I'_n} J(\cdot)$ denotes the gradient of the loss function $J(\cdot)$ with respect to I'_n , y_o is the original label, and ϵ is the perturbation budget. Researchers have proposed a variety of improved algorithms for IFGSM, e.g., the momentum iterative method (MI) [4] integrates a momentum term into the iterative process. Diverse inputs method (DI) [13] and translation-invariant method (TI) [14] leverage data augmentation to prevent the attack from overfitting a specific source model. Moreover, these enhanced schemes can be

* This work was supported by the network emergency management research special topic (no. WLYJGL2023ZD003), the Opening Project of Guangdong Province Key Laboratory of Information Security Technology (no. 2020B1212060078), Sichuan Science and Technology Program (no. 2022YFG0321).

integrated for even better transferability, e.g., Translation Invariant Momentum Diverse Inputs IFGSM (TMDI).

In addition to crafting AEs on the output layer, recent works have started to perturb the internal layers. [24, 25] try to maximize the distance between AE and the corresponding benign image on the feature space. [20] proposes to disrupt internal features according to their importance.

$$\arg \min_l \sum (\bar{\Delta}_k^l \cdot f_k(\mathbf{I}')), \quad s.t. \|\mathbf{I}' - \mathbf{I}\|_\infty \leq \epsilon \quad (2)$$

where $f_k(\cdot)$ denotes the feature maps from the k -th layer, and $\bar{\Delta}_k^l$ is the aggregate gradient used to measure the importance of the features. [21] improves [20] by using the integrated gradient [26] in measuring the feature importance, and [22] improves [20] by adopting a patch-wise mask in calculating aggregate gradients. Unlike the output-level attacks, extending feature-level attacks to the targeted mode is not trivial because representing the target class as a single point in an internal layer is difficult.

2.2. Transferable targeted attack

A targeted attack misguides a classification model to a specific label y_t as whatever the attacker intends, i.e., $f(\mathbf{I}') = y_t$. It is not a simple extension of its untargeted counterpart. There are at least two additional challenges unique to targeted attacks. The first is gradient vanishing [10, 11], i.e., the gradient decreases as the attack progresses. The other one is the restoring effect of y_o and other high-confidence labels when an AE is transferred to an unseen model [10, 12]. Hence, tailored considerations are required for transferable targeted attacks.

[10] replaces traditional cross-entropy (CE) loss with the Poincare distance loss to address the decreasing gradient problem and introduces a triplet loss to push the attacked image away from y_o . [11] uses the Logit loss in the attack and reports better transferability than the CE loss.

$$L_{Logit} = -l_t(\mathbf{I}') \quad (3)$$

where $l_t(\cdot)$ denotes the logit output with respect to y_t . Another non-trivial contribution of [11] is pointing out that targeted attacks need significantly more iterations to converge than untargeted ones. [12] argues that not only the original label y_o , but also other high-confidence labels should be suppressed for better transferability. Such an idea can be realized by updating AEs according to the following direction:

$$\nabla(l_t(\mathbf{I}') - \beta_1 l_o(\mathbf{I}')) - \beta_2 \nabla(\sum_{i=0}^{N_h} l_{high-conf,i}(\mathbf{I}')) \perp \quad (4)$$

where the first term is used to enhance the confidence of y_t and suppress y_o simultaneously. The second term is used to suppress other high-confidence labels. ‘ \perp ’ denotes only the orthogonal component (to the first term) is kept.

In addition to the simple transferable attacks reviewed above, resource-intensive attacks require training auxiliary target-class-specific classifiers or generators on additional data for better transferability. In the feature distribution attack [8], a light-weight, one-versus-all classifier is trained for each target class y_t at each specific layer to predict the probability that a feature map is from class y_t . [9] trains an input-

adaptive generator to synthesize targeted perturbation and achieves state-of-the-art transferability. However, a dedicated generator must be learned for every (*source model*, *target class*) pair in [9]. Henceforth, we denote the traditional CE loss-based attack, the Po+Trip loss-based attack [10], the logit loss-based attack [11], the high-confidence suppressing attack [12], and the transferable targeted perturbation [9] as CE, Po+Trip, Logit, SupHigh, and TTP, respectively.

3. PROPOSED SCHEME

3.1. Motivation

It is well-accepted that attacking the feature space can alleviate an AE’s overfitting issue (to the source model), thus improving its transferability across models. In the untargeted scenario, a feature space attack can be realized by pushing AE away from the clean image in the feature space. However, as the saying goes, *it’s easier to pull down than to build up*. In the targeted mode, there is no single point which perfectly represents y_t in the feature space that we can pull closer to. This challenge is partially addressed in [8] by training a one-versus-all auxiliary classifier for each y_t . However, this strategy is somewhat impractical in situations where the number of classes is enormous. The above challenges raise the question: *Can the targeted transferability of simple iterative attacks be increased via feature-space modification without model training on additional data?*

We believe that AEs crafted by simple iterative attacks already have reasonably strong targeted attack abilities, which their nearly perfect white-box success rates can partially verify. Their transferability is expected to improve if we can alleviate the overfitting issue. To this end, we try to fine-tune a crafted AE in the feature space. Beginning with an AE (Fig. 1(a)) generated by the CE attack with TMDI augmentation ($y_t = \text{‘grey owl’}$, $\epsilon = 16$), we perturb it in the last layer of the third block of the source model ResNet50 (Res50) [27] according to a targeted version of (2).

$$\arg \max_{\mathbf{I}'_{ft}} \sum (\bar{\Delta}_k^l \cdot f_k(\mathbf{I}'_{ft})), \quad s.t. \|\mathbf{I}'_{ft} - \mathbf{I}\|_\infty \leq \epsilon \quad (5)$$

Fig. 1(b) shows \mathbf{I}'_{ft} ’s confidence of ‘grey owl’ as functions of iteration number. Although the curves corresponding to

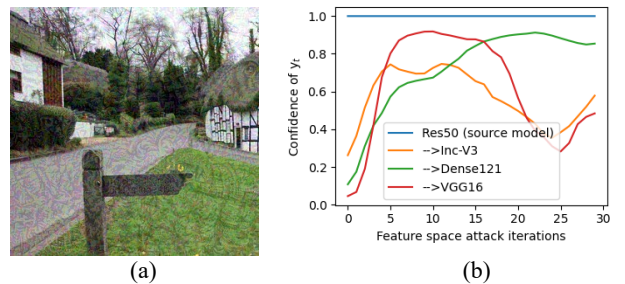


Fig. 1. The overfitting issue is alleviated after feature space fine-tuning. The target class is ‘grey owl’ and the source model is Res50. (a) The AE, (b) the trend of the confidence with respect to ‘grey owl’ as fine-tuning progress. The step size is one.

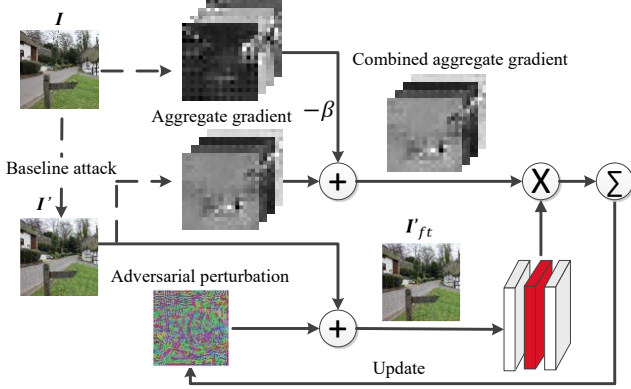


Fig. 2. Overview of feature space fine-tuning. Given an AE crafted by a baseline attack, its feature maps extracted from an internal layer (red block) are further optimized according to Eq. (7).

different target models differ significantly, they all develop towards higher confidence in the early stage, which means a few iterations of fine-tuning may help alleviate the overfitting issue of AEs crafted by the baseline attack. Based on this delightful observation, in the next section, we propose fine-tuning a simple iterative attack-generated AE in the feature space to improve its targeted transferability.

3.2. Feature space fine-tuning

Our proposed method is shown in Fig. 2. Starting from a benign image I , an AE I' is first generated by a baseline attack, e.g., CE or Logit, for N iterations. Next, we calculate the aggregate gradient $\bar{\Delta}_k^{I',t}$ to y_t , from the k -th layer of the source model. Following the idea of suppressing the original label y_o [10, 12], we also calculate the aggregate gradient $\bar{\Delta}_k^{I,o}$, with respect to y_o , from I . Then, $\bar{\Delta}_k^{I',t}$ and $\bar{\Delta}_k^{I,o}$ are combined to guide the subsequent feature space fine-tuning.

$$\bar{\Delta}_{k,combine} = \bar{\Delta}_k^{I',t} - \beta \bar{\Delta}_k^{I,o} \quad (6)$$

where β is a predefined weight used to balance these two terms. We set $\beta = 0.2$, following [12]. Finally, fine-tune I'

Algorithm 1 Feature space fine-tuning

Input: A benign image I with original label y_o ; target label y_t .

Parameter: Iterations N for baseline attack, N_{ft} for fine-tuning.

Output: Adversarial image I'_{ft} .

1. Mount a baseline attack for N iterations, and obtain an AE I' .
2. Calculate aggregate gradient $\bar{\Delta}_k^{I',t}$ from I' , and $\bar{\Delta}_k^{I,o}$ from I .
3. Obtain the combined aggregate gradient $\bar{\Delta}_{k,combine}$ as (6).
4. Fine-tune I' as (7), for N_{ft} iterations and obtain I'_{ft} .

for N_{ft} iterations, $N_{ft} \ll N$, with the optimization objective:

$$\operatorname{argmax}_{I'_{ft}} \sum (\bar{\Delta}_{k,combine} \cdot f(I'_{ft})), \quad s.t. \|I'_{ft} - I\|_{\infty} \leq \epsilon \quad (7)$$

In this way, the features contribute to y_t are encouraged, and those contribute to y_o are suppressed. **Algorithm 1** summarizes the entire process.

4. EXPERIMENTAL RESULTS

We compare the proposed method with four simple iterative attacks: CE [23], Po+Trip [10], Logit [11], SupHigh [12], and the current state-of-the-art generative attack, TTP [9]. All the iterative schemes start with the TMDI attack.

4.1. Experiment Settings

Dataset. Our experiments are conducted on the ImageNet-compatible dataset comprised of 1000 images [28]. All these images are cropped to 299×299 pixels before use.

Networks. Since transferring across different architectures is more challenging, we use four pretrained models of diverse architectures: Inceptionv3 (Inc-v3) [29], Res50, DenseNet 121 (Dense121) [30], and VGG16bn (VGG16) [31] as in [11] to evaluate AEs' transferability.

Parameters. For all competitors, the perturbations are restricted by L_{∞} norm with $\epsilon = 16$, and the step size is set as 2. Fine-tuning inevitably increases computational complexity even though $N_{ft} \ll N$. To make the running time of with/without fine-tuning comparable, we set the total

Table 1. Targeted transfer success rate (%) without/with fine-tuning, in the single-model, random-target scenario. Best results are in **bold**.

Attack	Source Model: Res50			Source Model: Dense121			Source Model: VGG16			Source Model: Inc-v3		
	→Inc-v3	→Dense121	→VGG16	→Inc-v3	→Res50	→VGG16	→Inc-v3	→Res50	→Dense121	→Res50	→Dense121	→VGG16
CE	3.9/ 9.0	44.9/ 60.4	30.5/ 49.3	2.3/ 13.2	19.0/ 45.3	11.3/ 34.8	0.0/0.0	0.3/ 2.8	0.5/ 3.3	1.8/ 4.7	2.1/ 7.8	1.5/ 4.0
Po+Trip	7.1/ 12.9	57.5/ 68.1	36.3/ 50.8	2.5/ 8.9	15.2/ 37.6	9.2/ 29.7	0.1/ 0.2	0.6/ 2.9	0.6/ 4.3	1.7/ 5.0	3.3/ 9.4	1.6/ 4.9
Logit	9.1/ 15.8	70.0/ 75.3	61.9/ 64.1	7.8/ 15.1	42.6/ 56.7	37.1/ 49.3	0.8/ 1.1	10.2/ 15.5	13.6/ 15.1	2.4/ 6.3	3.6/ 10.2	2.2/ 7.7
SupHigh	9.6/ 16.3	74.9/ 75.7	63.5/ 69.8	8.7/ 15.9	48.1/ 61.6	40.5/ 52.2	0.8/ 2.7	11.2/ 16.2	13.6/ 19.9	2.3/ 5.9	4.5/ 10.3	2.2/ 9.6

Table 2. Targeted transfer success rate (%) without/with fine-tuning, in the single-model, most difficult-target scenario.

Attack	Source Model: Res50			Source Model: Dense121			Source Model: VGG16			Source Model: Inc-v3		
	→Inc-v3	→Dense121	→VGG16	→Inc-v3	→Res50	→VGG16	→Inc-v3	→Res50	→Dense121	→Res50	→Dense121	→VGG16
CE	1.3/ 3.1	25.8/ 45.3	15.0/ 29.7	1.2/ 6.1	6.5/ 23.4	3.6/ 19.2	0.0/0.0	0.0/ 1.4	0.0/ 1.2	2.4/ 5.9	4.2/ 7.8	2.3/ 5.0
Po+Trip	2.8/ 5.3	40.5/ 47.6	20.5/ 30.8	0.9/ 4.2	6.1/ 21.8	2.5/ 17.7	0.0/0.0	0.1/ 1.7	0.0/ 1.1	2.4/ 6.1	4.1/ 7.5	2.7/ 6.3
Logit	3.6/ 6.5	51.6/ 53.1	38.6/ 44.3	3.5/ 8.3	22.7/ 41.6	18.3/ 37.5	0.3/ 0.4	2.8/ 8.9	7.0/ 8.5	3.8/ 8.0	5.5/ 10.5	3.2/ 7.9
SupHigh	4.0/ 7.1	54.5/ 55.9	41.6/ 45.2	4.0/ 8.6	24.5/ 43.3	21.2/ 40.4	0.1/ 0.3	3.9/ 10.1	6.8/ 9.4	4.0/ 8.2	4.9/ 10.6	3.4/ 10.2

iteration number $N=200$ for the baseline attacks without fine-tuning, and set $N=160$, $N_{ft}=10$ when fine-tuning is enabled. For the fine-tuning layer k , we choose the middle layer, following [20, 21]. Specifically, we select to attack *Mixed_6b* for Inc-v3, the last layer of the third block for Res50 and Dense121, and *Conv4_3* for VGG16. Due to page limitation, we leave the ablation study on N_{ft} , k , and aggregate gradient method, and the result of data-free targeted UAP [11] in the supplementary file: *TA_feature_FT/supp.pdf*.

4.2. Single-model transfer

Table 1 reports the targeted transferability (random-target) across different models. All the baseline attacks benefit from the proposed feature space fine-tuning. The improvement is particularly significant for the CE attack. For example, when transferring from Dense121 to VGG16, the success rate is approximately tripled after fine-tuning. Another significant improvement is the case of Inc-v3, which is reported to be challenging to transfer from or to in previous works [11, 12]. The last column shows that fine-tuning at least doubles the success rates when Inc-v3 is the source model.

As suggested in [11], we consider a worst-case transfer scenario in which the target label is the least likely one. Table 2 compares different attacks in such a challenging scenario. The improvement from fine-tuning is even more remarkable compared with the random-target scenario. Consistent with [12], we find that the success rates of the most difficult-target scenario are not necessarily lower than that of the random-target scenario when Inc-v3 is the source model before or after fine-tuning.

4.3. Ensemble transfer

Next, we evaluate the proposed fine-tuning scheme in the ensemble-model scenario. Specifically, we take turns taking out a model as the target and crafting AEs on the ensemble of the remaining models with equal weights. Note that there is no architectural overlap between the source and target models. Table 3 reports the targeted transferability in this scenario. Even though AE’s transferability in the ensemble-model scenario has been significantly improved compared with that in the single-model scenario, the proposed fine-tuning scheme is still helpful for it.

4.4. Iterative vs. generative attacks

Last, we compare the fine-tuned simple iterative attacks with the state-of-the-art generative attack, TTP [9]. TTP

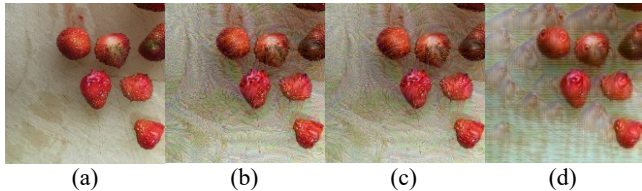


Fig. 3. The visual comparison of the AEs generated by different methods, $\epsilon = 16$. The target class is ‘hippopotamus’. (a) Original image, (b) Logit, (c) Logit+ft (ours), (d) TTP.

Table 3. Targeted transfer success rate (%) without/with fine-tuning, in the ensemble-model, random-target scenario, where ‘-’ indicates the hold-out model.

Attack	-Inc-v3	-Res50	-Dense121	-VGG16	Average
CE	24.4/ 40.1	53.5/ 57.6	77.3/ 78.7	76.8/ 79.3	58.0/ 63.9
Po+Trip	22.5/ 39.4	43.7/ 48.9	71.9/ 74.2	64.3/ 68.7	50.6/ 57.8
Logit	30.7/ 41.4	68.8/ 69.5	79.0 /78.9	81.6/ 82.1	65.0/ 68.0
SupHigh	34.8/ 43.5	72.4/ 72.5	81.8 /81.5	82.7/ 83.0	67.9/ 70.1

Table 4. Targeted transfer success rate (%) ($\epsilon = 8/16$) of fine-tuned iterative attacks vs. TTP, averaged over 10 targets. Source model: Res50.

Attack	→Inc-v3	→Dense121	→VGG16	Average
CE+ft	1.9/14.5	33.1/63.5	27.8/51.3	20.9/43.1
Po+Trip+ft	3.1/17.5	39.2/68.7	33.4/57.6	25.2/47.9
Logit+ft	3.4/18.6	48.4/77.9	46.3/75.7	32.7/57.4
SupHigh+ft	4.2/19.9	49.9 /78.3	49.4 / 76.9	34.5 /58.4
TTP	5.7 / 39.8	38.6/ 79.5	44.2/75.4	29.5/ 64.9

necessitates training a generator for each target label and each source model, which means 4×1000 generators are required to perform the random or most difficult-target attack as done in Section 4.2. Alternatively, we download ten pre-trained generators (Res50 being the discriminator during training) and follow the ‘10-Targets (all source)’ setting of [9], which corresponds to simple iterative attacks targeting ten selected classes with Res50 as the source model. We evaluate all competitors under different ϵ s. As shown in Table 4, fine-tuned state-of-the-art iterative attacks, Logit+ft and SubHigh+ft, achieve comparable ($\epsilon=16$) or even better ($\epsilon=8$) transferability to TTP. As pointed out in [11], the relatively poor transferability of TTP under a low budget is because it heavily relies on semantic patterns, which can be observed from Fig. 3(d). In contrast, the perturbation introduced by iterative methods resembles noise (Fig. 3(b, c)), which is less suspicious under human inspection. More examples are provided in the supplementary file.

5. CONCLUSION

We propose fine-tuning a given AE in the feature space to improve its targeted transferability. The proposed scheme delicately combines the idea of feature-level perturbation with simple iterative attacks, effectively alleviating the overfitting issue in existing methods without training target-specific classifiers or generators. The superiority of the proposed fine-tuning scheme is validated by integrating it with state-of-the-art iterative attacks in various transfer scenarios. Experimental results corroborate that feature space fine-tuning can boost the transferability of existing targeted attacks nontrivially and universally. Our results also verify that in targeted attack scenarios, simple iterative attacks have the potential to yield comparable transferability to resource-intensive methods.

6. REFERENCES

- [1] C. Szegedy, W. Zaremba, I. Sutskever, et al., “Intriguing properties of neural networks,” *International Conference on Learning Representations 2014*, arXiv: 1312.6199.
- [2] A. Madry, A. Makelov, L. Schmidt, et al., “Towards deep learning models resistant to adversarial attacks,” *International Conference on Learning Representations*, 2018.
- [3] S. J. Oh, M. Fritz and B. Schiele, “Adversarial image perturbation for privacy protection a game theory perspective,” *2017ICCV*, pp. 1491–1500.
- [4] Y. Dong, F. Liao, T. Pang, et al., “Boosting adversarial attacks with momentum,” *2018 IEEE/CVF conf. Computer Vision and Pattern Recognition*, pp. 9185–9193.
- [5] J. Lin, C. Song, K. He, et al., “Nesterov accelerated gradient and scale invariance for adversarial attacks,” *International Conference on Learning Representations*, 2020, arXiv: 1908.06281
- [6] C. Wan, B. Ye, F. Huang, “PID-based approach to adversarial attacks,” *the 35th AAAI Conference on Artificial Intelligence*, 2021, pp. 10033–10040.
- [7] Y. Liu, X. Chen, C. Liu, and D. Song, “Delving into transferable adversarial examples and black-box attacks,” *International Conference on Learning Representations*, 2017.
- [8] N. Inkawhich, K. J. Liang, L. Carin, and Y. Chen, “Transferable perturbations of deep feature distributions,” *International Conference on Learning Representations*, 2020.
- [9] M. Naseer, S. Khan, M. Hayat, et al., “On generating transferable targeted perturbations,” *Proceedings of IEEE International Conference on Computer Vision*, 2021, pp. 7688–7697.
- [10] M. Li, C. Deng, T. Li, et al., “Towards transferable targeted attack,” *2020 IEEE/CVF Conference on Computer Vision and Pattern Recognition*, pp. 638–646.
- [11] Z. Zhao, Z. Liu, and M. Larson, “On success and simplicity: a second look at transferable targeted attacks,” In *NeurIPS*, 2020.
- [12] H. Zeng, T. Zhang, B. Chen, et al., “Enhancing targeted transferability via suppressing high-confidence labels,” *International Conference on Image Processing*, 2023.
- [13] C. Xie, Z. Zhang, Y. Zhou, et al., “Improving transferability of adversarial examples with input diversity,” *2019 IEEE/CVF Conf. Computer Vision and Pattern Recognition*, pp. 2725–2734.
- [14] Y. Dong, T. Pang, H. Su, et al., “Evading defenses to transferable adversarial examples by translation-invariant attacks,” *2019CVPR*, pp. 4307–4316.
- [15] X. Wang and K. He, “Enhancing the transferability of adversarial attacks through variance tuning,” *2021CVPR*, pp. 1924–1933.
- [16] Y. Li, S. Bai, Y. Zhou, et al., “Learning transferable adversarial examples via ghost networks,” *the 34th AAAI Conference on Artificial Intelligence*, 2020, pp. 11458–11465.
- [17] M. Fan, W. Guo, and Z. Ying, et al., “Enhance transferability of adversarial examples with model architecture,” *2023ICASSP*.
- [18] Q. Huang, I. Katsman, Z. Gu, et al., “Enhancing adversarial example transferability with an intermediate level attack,” *2019 ICCV*, pp. 4732–4741.
- [19] Q. Li, Y. Guo, and H. Chen, “Yet another intermediate-level attack,” *2020ECCV*, pp. 241–257.
- [20] Z. Wang, H. Guo, Z. Zhang, et al., “Feature importance-aware transferable adversarial attacks,” *2021 IEEE/CVF International Conference on Computer Vision*, pp. 7619–7628.
- [21] J. Zhang, W. Wu, J. Huang, et al., “Improving adversarial transferability via neuron attribution-based attacks,” *2022 CVPR*, pp. 14973–14982.
- [22] Y. Zhang, Y. Tan, T. Chen, et al., “Enhancing the transferability of adversarial examples with random patch,” *IJCAI2022*, pp. 1672–1678.
- [23] A. Kurakin, I. Goodfellow, S. Bengio, “Adversarial examples in the physical world,” *Proceedings of Int. Conf. Learning Representations*, 2016. arXiv: 1607.02533.
- [24] W. Zhou, X. Hou, Y. Chen, et al., “Transferable adversarial perturbations,” in *ECCV*, pp. 452–467, 2018.
- [25] M. Naseer, S. Khan, S. Rahman, and F. Porikli, “Task-generalizable adversarial attack based on perceptual metric,” arXiv: 1811.09020, 2018.
- [26] M. Sundararajan, A. Taly, and Q. Yan, “Axiomatic attribution for deep networks,” in *International Conference on Machine Learning*, pp. 3319–3328, 2017.
- [27] K. He, X. Zhang, S. Ren, et al., “Deep residual learning for image recognition,” *2016CVPR*, pp. 770–778.
- [28] https://github.com/cleverhans-lab/cleverhans/tree/master/cleverhans_v3.1.0/examples/nips17_adversarial_competition/datas et
- [29] C. Szegedy, V. Vanhoucke, S. Ioffe, et al., “Rethinking the inception architecture for computer vision,” *2016CVPR*, pp. 2818–2826.
- [30] G. Huang, Z. Liu, V. Laurens, and K. Q. Weinberger, “Densely connected convolutional networks,” *2017CVPR*, pp. 2261–2269.
- [31] K. Simonyan, A. Zisserman, “Very deep convolutional networks for large-scale image recognition,” *International Conference on Learning Representations*, 2015.

Enhancing targeted transferability via feature space fine-tuning: supplementary material

Hui Zeng, Biwei Chen, and Anjie Peng

The supplementary document consists of five parts of content: A) Comparison with ILA [1], ILA++ [2, 3]; B) Ablation study on N_{ft} and k ; C) Visual comparison; D) Date-free targeted Universal adversarial perturbation (UAP); E) Alternative methods for calculating aggregate gradient.

A Comparison with existing fine-tuning methods

Several novel fine-tuning methods in untargeted attack have been proposed in the past few years. For instance, ILA maximizes the scalar projection of the adversarial example on the direction $f_l(I') - f_l(I)$, where $f_l(O)$ is the feature presentation in the l -th layer. ILA++ takes advantage of the directional guides gathered at each step of the baseline attack for a more stable guide direction. A straightforward question is:

Is the proposed method merely a targeted version of existing fine-tuning methods [1, 2, and 3]?

To answer this question, we first take a schematic diagram to illustrate the difference between the proposed method and the targeted version of ILA. As shown in Fig. 1, although both fine-tuning schemes start from an attacked image I' , the following directions are different. ILA is guided by $f_l(I') - f_l(I)$, whereas the proposed method is guided by $f_l(I')$. Such a difference embodies our unique considerations for targeted attacks:

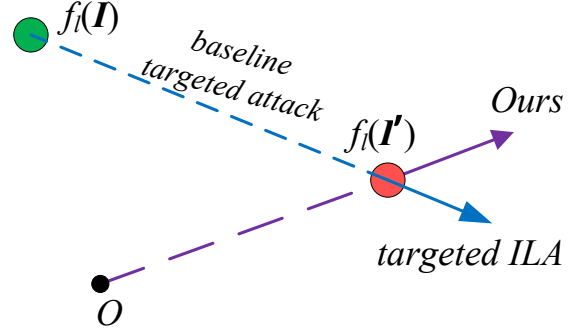


Fig. 1. Illustration of the difference between the proposed method and targeted ILA. ‘O’ represents the origin.

1) ILA is initially designed for untargeted attacks. Hence, it prioritizes moving away from the original class. In contrast, our strategy focuses more on increasing the probability of the target class.

2) We believe that the image content I and the adversarial perturbation $I' - I$ are closely intertwined in the feature space. Thus, $f_l(I') - f_l(I)$ may not be a better guide than $f_l(I')$.

Then, we experimentally compare the proposed method with targeted ILA. The experimental setup (N_{ft}, k) of the targeted ILA is the same as the proposed method. Tables 1 and 2 report the targeted success rates of compared schemes under the random-target and most difficult-target scenarios, respectively. The proposed method triumphs over targeted ILA by a clear margin.

Table 1. Comparison of fine-tuning with ILA and the proposed method. Targeted transfer success rates (%) in the single-model, random-target scenario. Dominant results are in **bold**.

Attack	Source Model: Res50			Source Model: Den121			Source Model: VGG16			Source Model: Inc-v3			AVG
	→Inc-v3	→Den121	→VGG16	→Inc-v3	→Res50	→VGG16	→Inc-v3	→Res50	→Den121	→Res50	→Den121	→VGG16	
CE	3.9	44.9	30.5	2.3	19.0	11.3	0.0	0.3	0.5	1.8	2.1	1.5	9.8
CE+ILA	10.6	60.3	44.2	11.5	35.6	29.3	0.0	1.6	3.2	2.6	4.3	2.8	17.2
CE+ f_l (ours)	9.0	60.4	49.3	13.2	45.3	34.8	0.0	2.8	3.3	4.7	7.8	4.0	19.6

Table 2. Comparison of fine-tuning with ILA and the proposed method. Targeted transfer success rates (%) in the single-model, most difficult-target scenario.

Attack	Source Model: Res50			Source Model: Den121			Source Model: VGG16			Source Model: Inc-v3			AVG
	→Inc-v3	→Den121	→VGG16	→Inc-v3	→Res50	→VGG16	→Inc-v3	→Res50	→Den121	→Res50	→Den121	→VGG16	
CE	1.3	25.8	15.0	1.2	6.5	3.6	0.0	0.0	0.0	2.4	4.2	2.3	5.2
CE+ILA	3.6	42.4	28.9	5.2	19.5	14.7	0.0	0.0	0.0	4.3	4.7	5.0	10.7
CE+ f_l (ours)	3.1	45.3	29.7	6.1	23.4	19.2	0.0	1.4	1.2	5.9	7.8	5.0	12.3

- [1] Q. Huang, I. Katsman, Z. Gu, et al., “Enhancing adversarial example transferability with an intermediate level attack,” *2019ICCV*, pp. 4732–4741.
- [2] Q. Li, Y. Guo, and H. Chen, “Yet another intermediate-level attack,” *2020ECCV*. pp. 241–257.
- [3] Y. Guo, Q. Li, and W. Zuo, et al., “An intermediate-level attack framework on the basis of linear regression,” *2022TPAMI*.

B Ablation study

1) **Influence of the fine-tuning iteration N_{ft} .** We study the influence of N_{ft} on the transfer success rate in the single-model, random-target scenario, with the source model fixed as Res50. The optimal N_{ft} varies from 10 to 15 when the baseline attack is CE (Fig. 2(a)) and from 5 to 10 when the fine-tuning is based on Logit (Fig. 2(b)). This can be explained as follows. A relatively weak attack, e.g., CE, has greater potential for improvement and thus needs more iterations of fine-tuning. In contrast, a relatively strong attack, Logit or model-ensemble, is more suitable for less fine-tuning. In our study, we set $N_{ft} = 10$ for all attacks and in all scenarios for simplicity. Fig. 2 indicates that $N_{ft} = 10$ is almost always dominant $N_{ft} = 0$ that represents no fine-tuning.

2) **Influence of the fine-tuning layer k .** Next, we study the influence of target layer k in fine-tuning on the transfer success rate. In this experiment, we fix the other parameters of the proposed method and select a few internal layers for each source model. Fig. 3(a), (b), and (c) report the transferability of adversarial examples crafted on source models Res50, Dense121, and Inc-V3, respectively. The main takeaway is that fine-tuning on a middle layer is helpful to transferability. This finding is consistent with previous works that early layers are usually data-specific, whereas later ones are model-specific. Based on the above considerations, we select to attack *Mixed_6b* for Inc-v3, the last layer of the third block for Res50 and Dense121, and *Conv4_3* for VGG16 in this study.

B Visual comparison

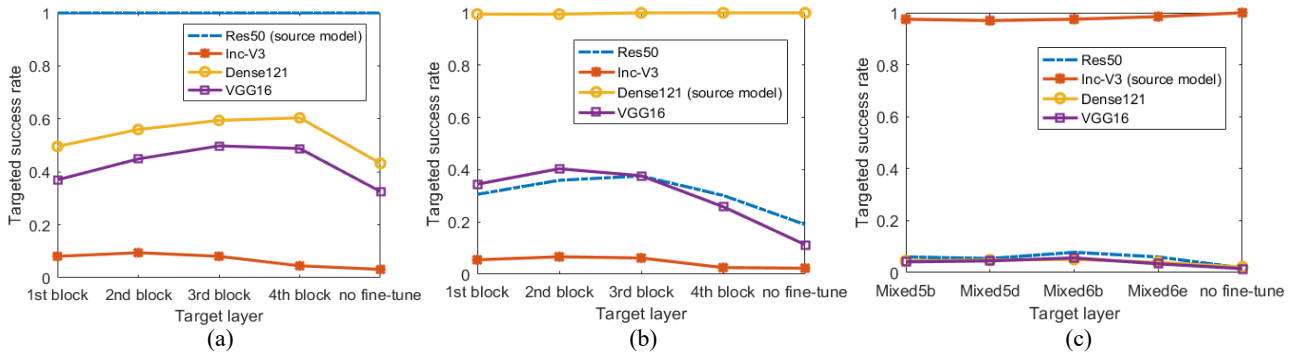


Fig. 3. Effect of target layer on AEs’ transferability. The baseline attack is CE. The source models are Res50 (a), Dense121 (b), and Inc-V3 (c), respectively.

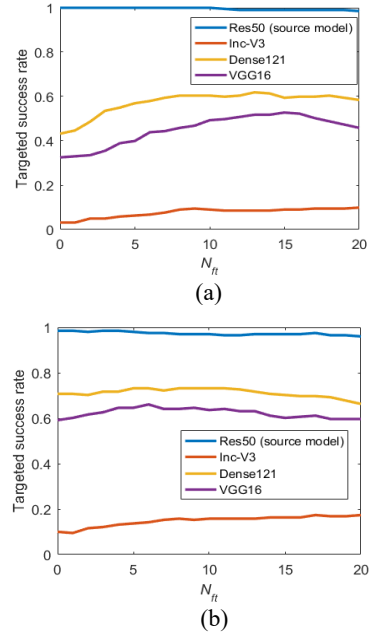


Fig. 2. Effect of N_{ft} on AEs’ transferability. The source model is Res50. The baseline attack is CE (a) and Logit (b).

Besides the example in the paper, we provide additional examples in this file. Fig. 4 shows AEs targeted to ‘grey owl,’ and Fig. 5 shows AEs targeted to ‘hippopotamus.’ While the perturbation introduced by the iterative methods resembles noise, that introduced by TTP is more semantically-aligned.

C Data-free targeted UAP

Targeted UAP is a particular type of perturbation that can drive multiple clean images into a given class y_t . Among the methods for crafting targeted UAP, we are particularly interested in the data-free approach, which does not require additional training data. Precisely, we use a mean image (all entrances of which equal 0.5) as the start point and mount a targeted attack for 200 iterations to obtain a targeted UAP ($\epsilon = 16$) with different simple iterative methods. Then, the obtained UAP is applied to all 1000 images in our dataset.

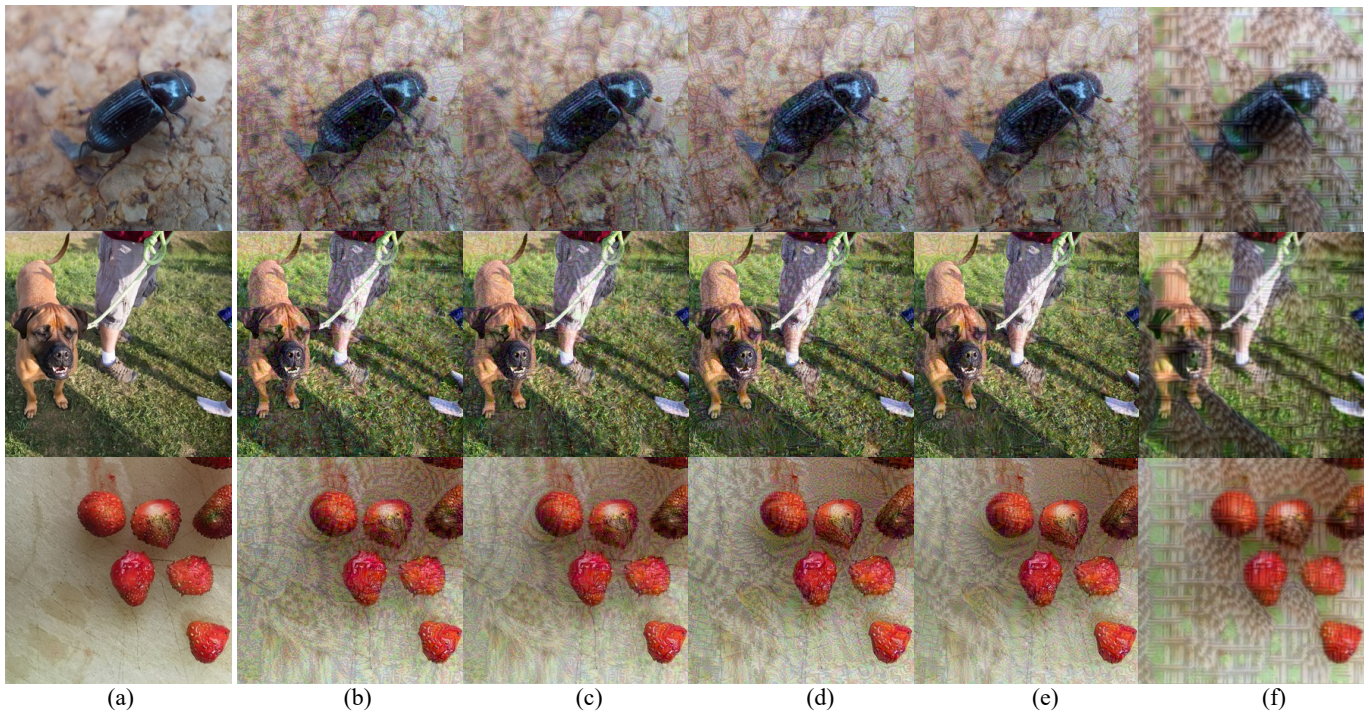


Fig. 4. The visual comparison of the AEs generated by different methods, $\epsilon = 16$. The target class is ‘grey owl’. (a) Original image, (b) CE, (c) CE+ft (proposed), (d) Po+Trip, (e) Po+Trip+ft (proposed), (f) TTP.

Table 3 reports the success rates averaged over 100 classes ($y_t = 0:99$). It is observed that feature space fine-tuning consistently improves the baseline attacks. Combining the results of the paper, we can conclude that the proposed fine-tuning scheme improves AEs’ transferability not only across models but also across input images. Fig. 6 presents examples

of targeted UAPs generated with different methods. It is observed that the UAPs are less noisy after feature space fine-tuning.

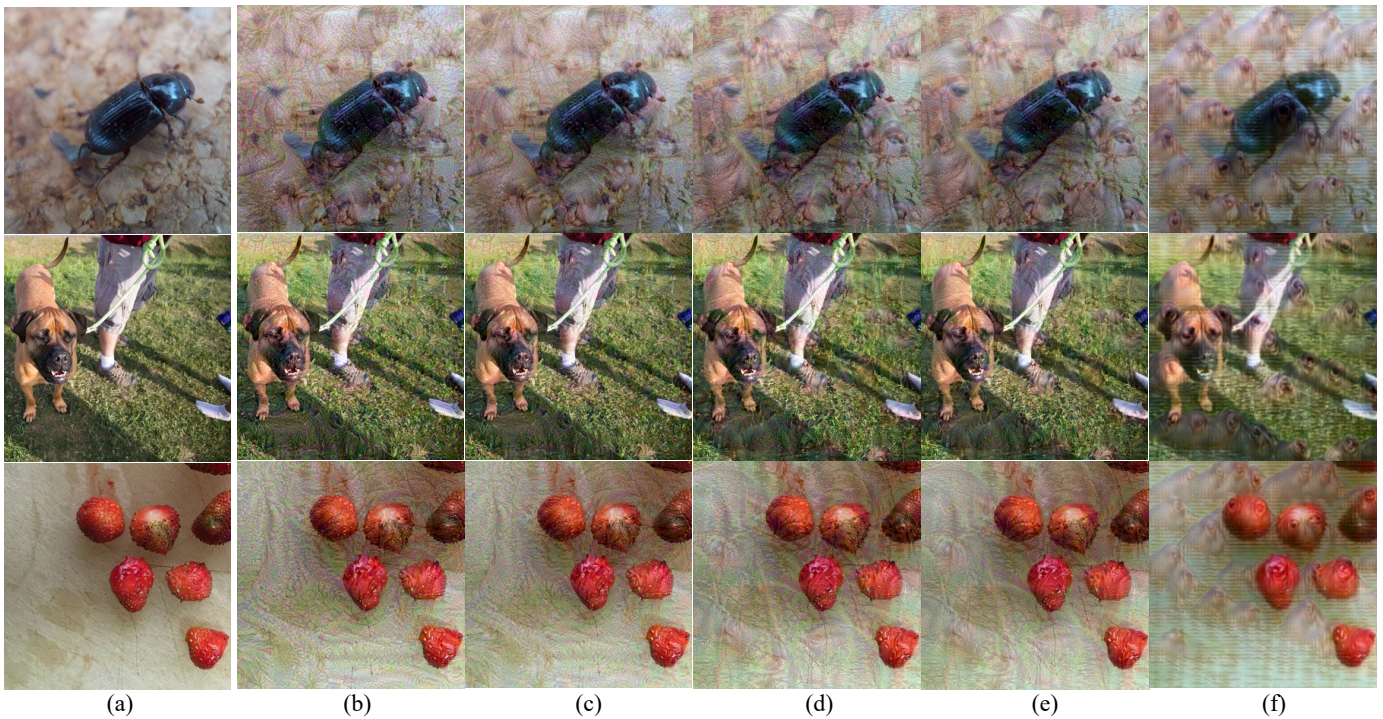


Fig. 5. The visual comparison of the AEs generated by different methods, $\epsilon = 16$. The target class is ‘hippopotamus’. (a) Original image, (b) Logit, (c) Logit+ft (proposed), (d) SupHigh, (e) SupHigh+ft (proposed), (f) TTP.

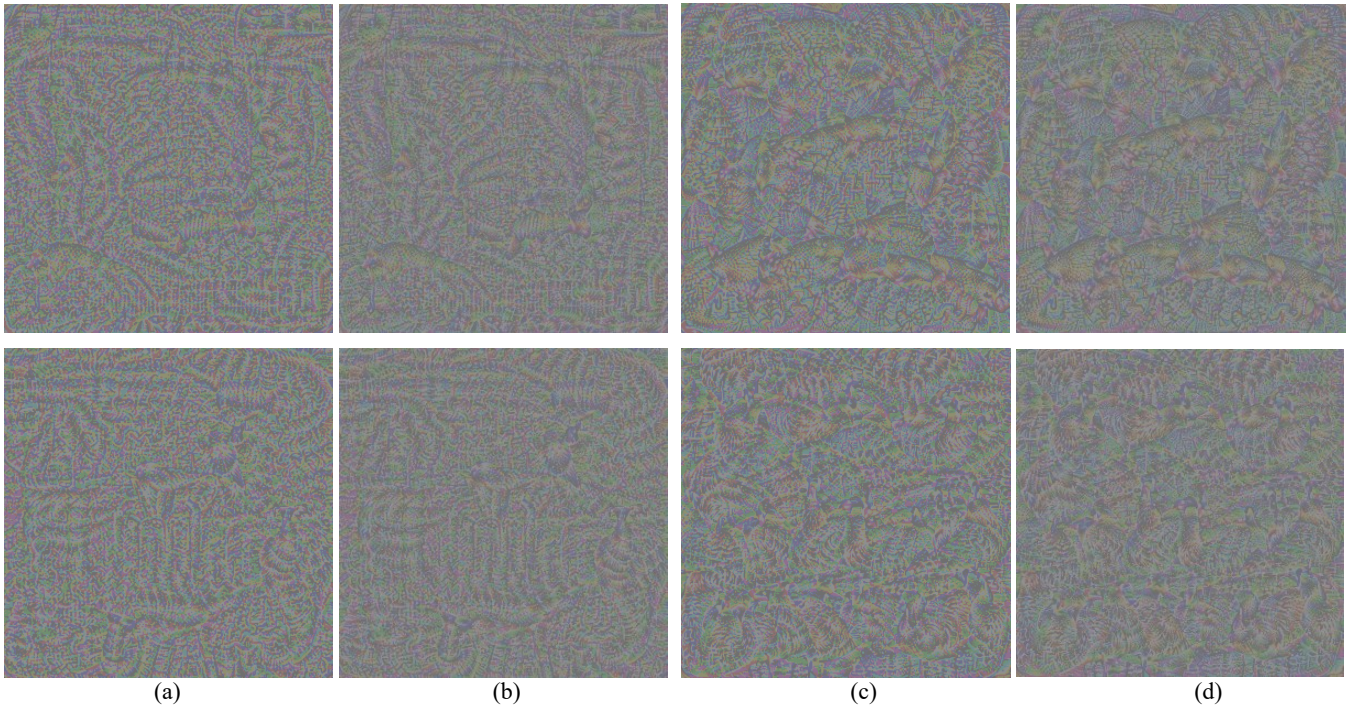


Fig. 6. Data-free targeted UAPs ($\epsilon = 16$, VGG16) generated by different methods. The target class is ‘tench’ for the first row, and ‘goose’ for the second row. (a) CE, (b) CE+ft, (c) Logit, (d) Logit+ft (proposed).

Table 3. Success rates (%) of the data-free UAPs with $\epsilon = 16$. Without/with fine-tuning. Dominant results are in **bold**.

Attack	Res50	Dense121	VGG16	Inc-v3
CE	8.1/ 15.1	8.0/ 13.1	19.2/ 34.6	1.9/ 2.4
Logit	20.7/ 24.6	17.5/ 18.8	64.9/ 66.3	3.6/ 4.7

D Alternative aggregate gradients

This subsection investigates the effect of the method of calculating aggregate gradients on the proposed fine-tuning scheme. Fig. 7 compares the transferability of AEs (under the random-target and most difficult-target scenarios, $\epsilon = 16$) when the aggregate gradient is generated with FIA [4] and RPA

[5]. Unlike FIA, which adopts a pixel-wise mask, RPA adopts a patch-wise mask in calculating aggregate gradients. For a fair comparison, we set the ensemble number $N=30$ for both FIA and RPA. Our results show that the more advanced RPA indeed improves the transferability slightly in most cases. This result indicates the proposed method can be further improved by incorporating more advanced aggregate gradient methods. In the paper, we use FIA to generate the aggregate gradient for simplicity.

[4] Z. Wang, H. Guo, Z. Zhang, et. al., “Feature importance-aware transferable adversarial attacks,” *ICCV2021*, pp. 7639–7648.

[5] Y. Zhang, Y. Tan, T. Chen, et. al., “Enhancing the transferability of adversarial examples with random patch,” *IJCAI2022*, pp. 1672–1678.

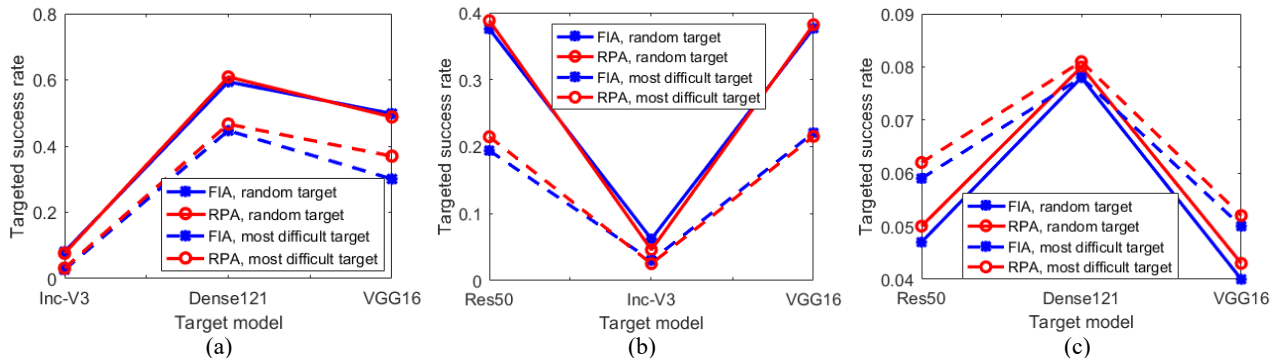


Fig. 7. Comparison AEs’ transferability when the aggregate gradients are generated with FIA and RPA. The baseline attack is CE. The source models are Res50 (a), Dense121 (b), and Inc-V3 (c), respectively.